

## The Preparation of Titania Nano Crystals and Silica-Titania Core-Shell Particles through Peptization Process

Jung Soo Kim, Soo Jung Kim, Eun Gu Jung, Hwan Hui Yun and Sang Man Koo\*

Hybrid Nano Particle Laboratory, Department of Chemical Engineering, Hanyang University, Seoul, 133-791, Korea

Monodispersed silica-titania core-shell particles with a controllable thickness and crystallinity were prepared by a simple peptization process in an aqueous acidic solution without the use of any external additives such as polyelectrolytes, polymers, and surfactants. The crystallinity of the titania nanocrystals coated on core-shell particles was controlled by adjusting the pH of the reaction medium. The shell thickness was found to increase as the reaction temperature, time, and the amount of Ti source material were increased. As-prepared core-shell particles with a smooth surface roughness were transformed into core-shell particles covered with largely grown titania crystals with different phases depending on the heat treatment temperature. The morphology and phase development of the particles were characterized via SEM, TEM, and XRD.

**Key words:** Silica, Titania, Nanocrystals, Core-shell particles, Peptization.

### Introduction

Titania ( $\text{TiO}_2$ ) is a chemically stable and environmentally benign substance that exhibits several interesting properties. It has generally been employed not only as a white pigment, but also as a UV protection reagent due to its high refractive index and strong absorption energy band in the UV region [1-4]. Recently, nano-sized titania particles have received an increasing amount of attention in the fields of photocatalysis, solar energy conversion, and environmental sensors [5-7]. Smaller titania nanocrystals have an increased surface-to-volume ratio, which can in turn generate more active sites for photochemical reactions. In addition, the semiconducting properties of titania have to be controlled by adjusting the band gap of the material toward visible wavelengths through the introduction of dopants and inducing structural modifications so as to form various morphologies and microstructures [8-9]. It has been well-documented that the morphology of titania is strongly dependent on its crystalline structure, which occurs naturally as three main crystalline phases (brookite, anatase, and rutile).

Titania particles that are supported on metal oxide spheres have been intensively investigated for their use in photocatalysis, photonics, and toner applications [5, 10]. It has been found that titania crystals on the surface of support materials have exhibited a significant enhancement in their stability and surface area when compared to unsupported crystals [11]. Among the various metal oxide cores, silica has been the most

studied material because of its simple and low cost production process, as well as its diverse size range. Xing-cai and Peng prepared titania coated silica particles by a multistep method with titanium n-butoxide. Nakamura et al. synthesized silica-titania core shell particles using a layer-by-layer (LbL) templating method [12, 13]. However, most of the synthesis methods developed thus far involve rather complicated procedures and expensive polymers and surfactants. Recently, Lim et al. prepared monodispersed core-shell type silica-titania spherical particles using a simple sol-gel route [14]. The researchers impregnated hydrolyzed titanium alkoxide onto silica particles without using a polyelectrolyte and surfactant. However, a very long preparation time was required to obtain core-shell particles with a homogeneous coating of titania. In this paper we describe a facile peptization procedure for the preparation of monodispersed silica-titania core-shell particles with a controllable thickness and crystallinity. This method not only avoids complicated processes such as the layer-by-layer technique and polymer/surfactant grafting methods, it also reduces costs due to its short reaction time and the use of inexpensive reactants. The crystallinity of the titania nanocrystals coated on core-shell particles was controlled by adjusting the pH of the reaction medium. Optimum conditions for the formation of core-shell particles were established by systematically changing such reaction variables as the concentration, temperature, and time.

### Experimental

#### Chemicals

The following materials have been purchased commercially and were used without further purification: tetraethyl

\*Corresponding author: Sang Man Koo  
Tel : +82-2-2220-0527  
E-mail: sangman@hanyang.ac.kr

orthosilicate (98%, Aldrich), titanium isopropoxide (97%, Aldrich), nitric acid (62%, Junsei), ethyl alcohol (99.9%, J.T. Baker), ammonium hydroxide (29.2%, Mallinkrodt), and distilled water.

### The formation of titania nano crystals through peptization

In a typical peptization process, a specific amount of titanium isopropoxide (2 mL or 0.13 M) was added to 50 mL of distilled water with stirring. Within a few minutes, a white suspension was formed and then coagulated titanium oxide was precipitated. After filtration, the resulting titania gel was added to an aqueous nitric acid solution. The  $[H_3O^+]$  concentration of the acidic solution was adjusted in the range of  $0.07\text{ M} < [H_3O^+] < 1.05\text{ M}$  with the addition of 0.25 to 4 mL of nitric acid into 50 mL of distilled water. The resulting suspension was stirred for several hours (typically 4 hours) at a temperature of  $70^\circ\text{C}$ . Depending on the  $[H_3O^+]$  concentration and reaction temperature of the solution, a clear white to blue suspension was obtained which indicated the formation of nano-sized titania particles with different sizes and morphologies.

### The preparation of silica-titania core-shell particles

An amount of silica particles (1 wt.%), prepared by the Stöber process [15], was dispersed in 50 mL of distilled water with sonication. Coagulated titanium oxide precipitate (0.13 M) was added to this silica suspension. Acid-catalyzed peptization, as described above, was then carried out in the presence of the silica particles by adding aqueous nitric acid solutions with different  $[H_3O^+]$  concentrations ( $0.07\text{ M} < [H_3O^+] < 1.05\text{ M}$ ) at different heating temperatures. By controlling reaction variables such as the  $[H_3O^+]$  concentration, temperature, and silica concentration, silica-titania core-shell particles with different sizes and morphologies were successfully fabricated.

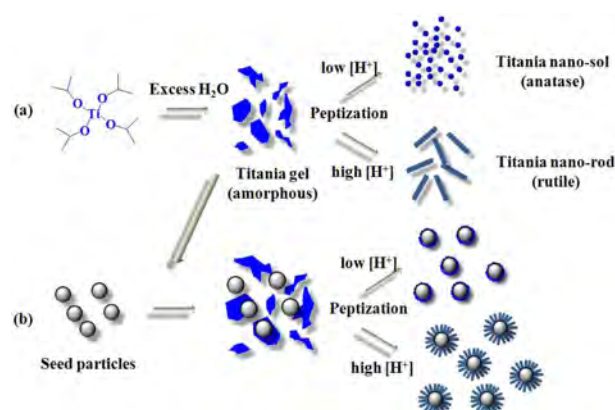
### Characterization

The size and morphology of the nano-sized titania particles and core-shell particles were determined via SEM (JSM-6701F, ZEOL) and TEM (LIBRA 120, CarlZeiss). The crystallinity of the fabricated particles was confirmed through X-ray diffractometry (XRD-6000X X-ray diffractometer, Shimadzu) with a  $\text{Cu-K}\alpha$  radiation source and a fixed power source (40 kV and 60 mA). The zeta potentials of the silica seed, titania nanocrystals, and the as-prepared core-shell particles were measured with a Model Zetasizer Nano ZS 90 (3 nm ~ 10  $\mu\text{m}$ ).

## Results and Discussion

### The formation of titania nano crystals through peptization

The formation of titania nano crystals through peptization



**Sch. 1.** The formation of (a) titania nanocrystals and (b) core-shell particles through peptization process.

is shown in Sch. 1. When titanium isopropoxide was added to an aqueous solution, rapid hydrolysis and condensation of mononuclear titanium alkoxides occurred and amorphous  $\text{TiO}_2 \cdot x\text{H}_2\text{O}$  aggregates containing a polymeric metal-oxo (Ti-O-Ti) network were precipitated (Sch. 1(a)) [16]. Under acidic peptization conditions, the breaking of Ti-O-Ti bonds in amorphous  $\text{TiO}_2 \cdot x\text{H}_2\text{O}$  led to the formation of Ti-OH and  $\text{Ti-OH}_2^+$  bonds in the structural units. As the process of acid peptization became more prevalent, more low molecular weight titanium aqua/hydroxide species such as oligomers and monomers were produced. These newly formed titanium oligomers and monomers were then bound together to form new Ti-O-Ti bonds by acid-catalyzed condensation and eventually produced titania nano crystals through a nucleation-growth mechanism. The size, structure, and morphology of the titania nano crystals could be controlled by adjusting the  $[H_3O^+]$  concentration and the reaction time during peptization. The effect of the  $[H_3O^+]$  concentration on the size and morphology of the titania nano crystals could be correlated to the solubility of the titania crystals at different acid concentrations. The morphologies and crystal structures of titania crystals at different  $[H_3O^+]$  concentrations are shown in Fig. 1. The smallest titania nano crystals with an anatase structure and a size of 3 ~ 5 nm could be obtained at a  $[H_3O^+]$  concentration of around 0.07 M. At this  $[H_3O^+]$  concentration, amorphous  $\text{TiO}_2 \cdot x\text{H}_2\text{O}$  was initially converted to the protonated penta-titanate intermediate H-titanate ( $\text{H}_2\text{Ti}_5\text{O}_{11} \cdot 3\text{H}_2\text{O}$ ) with a lamella structure [17]. As the reaction with acid proceeded further, dehydration between the Ti-OH bonds occurred and  $\text{TiO}_2$  crystals with new Ti-O-Ti bonds were formed. It is known that crystal lattices of H-titanate and anatase  $\text{TiO}_2$  have similar structural features such as four-edge sharing and zigzag ribbons [18, 19]. Therefore,  $\text{TiO}_2$  nano crystals with an anatase structure were formed from the peptization of amorphous  $\text{TiO}_2 \cdot x\text{H}_2\text{O}$  through a direct rearrangement of the crystal lattice [20]. As the  $[H_3O^+]$  concentration in the peptization process was increased, the size of the

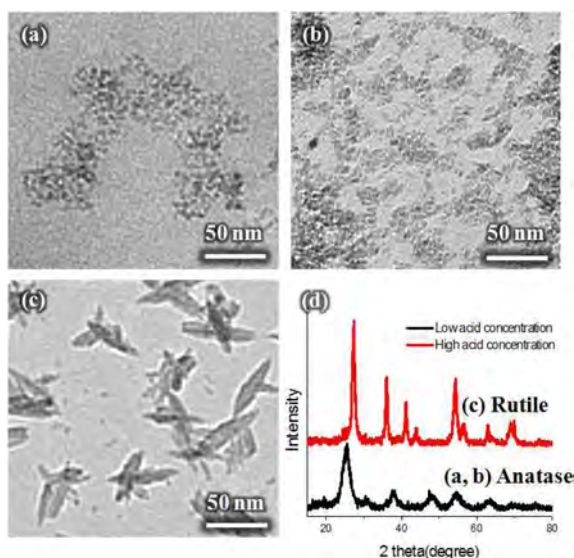


**Fig. 1.** TEM images (a, b, c) and XRD patterns (d) of titania nanocrystals prepared at different peptization conditions; temperature = 70 °C, reaction time = 4 hr, [Ti] = 0.13 M, (a)  $[H_3O^+] = 0.07$  M, (b)  $[H_3O^+] = 0.13$  M, (c)  $[H_3O^+] = 0.52$  M.

titania nano crystals slightly increased. The increase in the size of the anatase titania crystals could be explained by a growth mechanism that involves a dissolution/re-precipitation process. When the  $[H_3O^+]$  concentration in the peptization process was further increased to a value higher than 0.52 M, rod-shaped titania crystals with a rutile structure were obtained. At such a high  $[H_3O^+]$  concentration, even titania crystals with an anatase structure could be dissolved, while rod-shaped titania nano crystals with the more stable rutile structure were not dissolved.

#### The preparation of silica-titania core-shell particles

When the peptization of amorphous  $TiO_2 \cdot xH_2O$  occurred in the presence of silica particles, silica-titania core-shell particles were formed by the deposition of titania nano crystals onto the surface of the silica particles. This process is shown in Sch. 1(b). Similar to the peptization results described earlier, core-shell particles coated with anatase titania nano crystals were obtained at a relatively low  $[H_3O^+]$  concentration. However, to obtain core-shell particles with the silica/amorphous titania suspension, a slightly higher  $[H_3O^+]$  concentration of 0.13 M was required when compared to the concentration used for amorphous  $TiO_2 \cdot xH_2O$  alone. This may be explained by a scenario where some portion of the added  $[H_3O^+]$  was used to neutralize OH functional groups on the surface of the silica particles. In order to maintain a similar (or identical)  $[H_3O^+]$  concentration for the peptization reaction used earlier, a slight amount of excess  $[H_3O^+]$  has to be supplied to the suspension in order to compensate for the OH functional groups on the silica particles. The effect of the  $[H_3O^+]$  concentration on the formation of

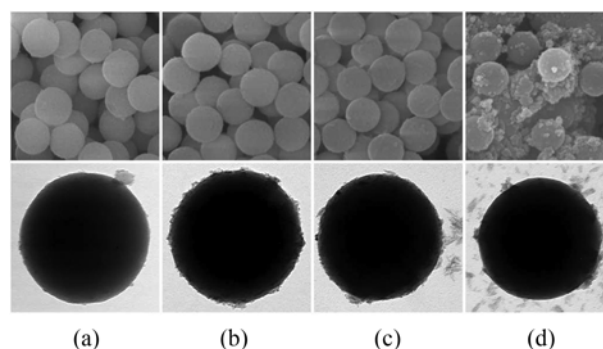


**Fig. 2.** SEM and TEM images for morphology changes in core-shell particles prepared at different reaction conditions; 1 wt.% silica seed (360 nm), [Ti] = 0.13 M, temperature = 70 °C, reaction time = 4 hr (a)  $[H_3O^+] = 0.07$  M, (b)  $[H_3O^+] = 0.13$  M, (c)  $[H_3O^+] = 0.52$  M, (d)  $[H_3O^+] = 1.05$  M

silica-titania core-shell particles is shown in Fig. 2. When excess  $[H_3O^+]$  was not added, for example  $[H_3O^+]$  concentration of 0.07 M was used, core-shell particles coated with incompletely peptized amorphous titania were obtained. Core-shell particles coated with completely peptized titania crystals could be obtained at a  $[H_3O^+]$  concentration of 0.13 M when 1 wt.% silica particles with a size of 360 nm were used as seed particles. Core-shell particles with rod-shaped titania crystals were obtained when the  $[H_3O^+]$  concentration of the suspension was higher than 0.52 M. When the  $[H_3O^+]$  concentration of the suspension was further increased to 1.05 M, uncoated rod-shaped rutile crystals were observed as well as core-shell particles. In this case, the higher  $[H_3O^+]$  concentration of the solution promoted the condensation rate, which in turn accelerated the formation of rod-shaped rutile crystals. Largely grown rutile crystals can then compete with silica particles as seed particles in the growth of titania nano crystals. XRD patterns of core-shell particles prepared at different  $[H_3O^+]$  concentrations did not show any discernible diffraction peaks. Only a broad peak around  $\theta = 23^\circ$  from the amorphous silica seed particles was observed. It seemed that the amount of titania particles coated on the core-shell particles was too small to exhibit any diffraction peaks. On the other hand, typical diffraction patterns from anatase and rutile structures were observed from titania nano crystals that were obtained as a by-product of each core-shell particle preparation process.

The reaction temperature had a strong effect on the coating thickness of the core-shell particles. TEM images that reveal the morphology changes in the core-shell particles at different reaction temperatures, times, and  $TiO_2 \cdot xH_2O$  concentrations are shown in Fig. 3. As the reaction temperature was increased, core-shell particles with a thicker shell and a relatively rough surface were obtained. Nearly uncoated silica particles were obtained when the reaction temperature was decreased as low as 50 °C as shown in Fig. 3-(1). At

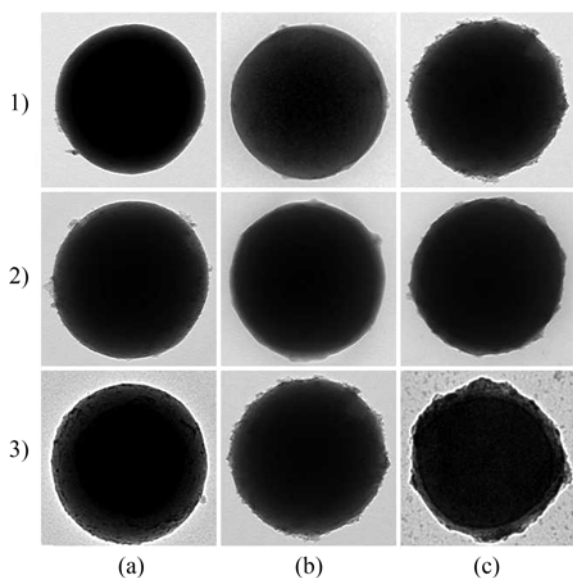


**Fig. 3.** Morphology changes in core-shell particles prepared at different reaction conditions; 1 wt.% silica seed (360 nm) and  $[H_3O^+] = 0.13$  M, 1)  $[Ti] = 0.13$  M, time = 4 hr, and temperature of (a) 50 °C (b) 65 °C, (c) 70 °C, 2)  $[Ti] = 0.13$  M, time = 10 hr, and temperature of (a) 50 °C, (b) 65 °C, (c) 70 °C, 3) time = 4 hr, temperature = 70 °C, and  $[Ti]$  of (a) 0.06 M (b) 0.13 M, (c) 0.26 M.

higher temperatures, the rate of peptization and condensation would be increased and the formation of agglomerate secondary titania nano crystals on the surface of the core-shell particles would be enhanced. On the other hand, the reaction time did not appear to have a significant effect on the formation of core-shell particles, although core-shell particles could be observed even at a reaction temperature of 50 °C when the reaction time was increased to 10 hours. When compared to particles prepared with a 4 hour reaction time, no significant difference was observed for core-shell particles prepared at temperatures higher than 65 °C for 10 hours as shown in Fig. 3-(2). It seemed that the formation of core-shell particles would be almost complete within a 4 hour reaction time above 65 °C. The effect of an amount of amorphous titania gel on the morphology of the core-shell particles was also investigated. As the concentration of  $TiO_2 \cdot xH_2O$  was increased, the shell thickness of the core-shell particles was higher. However, when the concentration of  $TiO_2 \cdot xH_2O$  was higher than 0.26 M, a mixture of core-shell particles and agglomerate titania started to appear (Fig. 3-(3)). Changes in the morphology and microstructure of the core-shell particles before and after calcination were investigated via electron microscopy and XRD analysis. As shown in Fig. 4, there was no discernible diffraction peak for all of the as-prepared core-shell regardless of the reaction conditions. Calcined core-shell particles with a well-developed diffraction pattern indicative of the rutile structure were obtained when a large amount of Ti source material and a temperature of 70 °C were

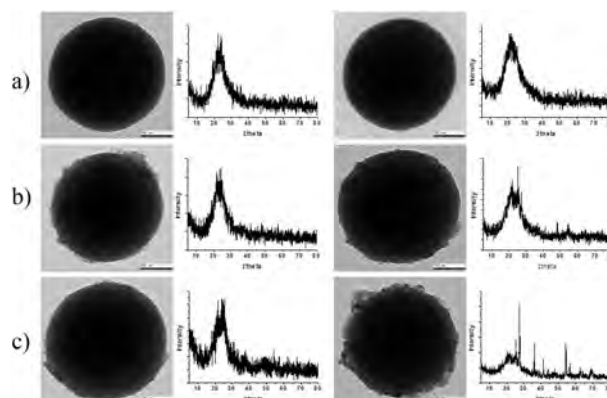


**Fig. 4.** TEM images and XRD patterns of core-shell particles before (left) and after heat treatment at 800 °C (right) with different reaction conditions; 1) peptization time = 15 hr, 2) temperature of (a) 65 °C and (b, c) 70 °C, 3) (a, b)  $[Ti]$  of 0.13 M and (c) 0.19 M.

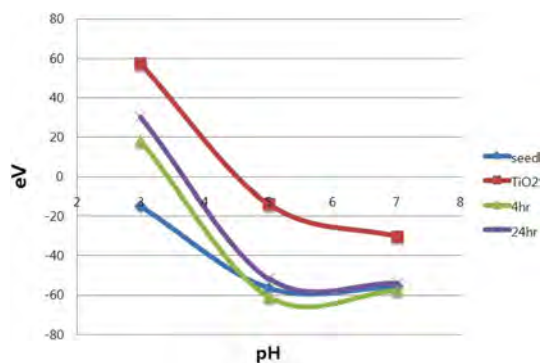


**Fig. 5.** Zeta potentials for silica seed, titania nanocrystals, and core-shell particles prepared with different reaction conditions.

employed. When the reaction temperature or the amount of Ti source material was decreased, a less-developed or no diffraction pattern was observed. It is believed that the appearance of XRD diffraction peaks was dependent not on the microstructure, but on the amount of titania nanocrystals on the surface of the core-shell particles. It has been confirmed that titania nano crystals with an anatase or rutile structure could be obtained at given reaction conditions through the peptization of amorphous titania,  $TiO_2 \cdot xH_2O$ . Therefore, it can be assumed that no diffraction peaks were observed because the amount and size of the titania crystals on the core-shell particles were too small to exhibit any noticeable XRD pattern. When either the reaction temperature or the concentration of Ti source material was increased, the amount of titania nanocrystals on the core-shell particles also increased. Such a scenario resulted in the largely grown secondary titania crystals observed in the TEM images. These largely grown secondary titania crystals exhibited a well-defined XRD pattern with a narrow peak width. Shown in Fig. 5 is the variation in the zeta potential at different pH values for the silica seed, titania nanocrystals, and as-prepared core-shell particles. As expected, an isoelectric point (IEP) for the core-shell particles coated with titania

nanocrystals lies between the IEP points for the silica seed particles and the titania nanocrystals. This point was shifted closer to that for the titania nanocrystals as the shell thickness of the core-shell particles was increased.

### Conclusions

In summary, a facile synthesis method for monodispersed silica-titania core-shell particles with a controllable thickness and crystallinity was developed. This technique involved the use of a peptization process in an aqueous acidic solution without employing external additives such as polyelectrolytes, polymers, and surfactants. The crystallinity of titania nanocrystals coated on core-shell particles was controlled by adjusting the pH of the reaction medium. As the  $[H_3O^+]$  concentration of the peptization medium increased from 0.07 M to 0.52 M, the structure of the titania was transformed from anatase to rutile. The shell thickness of the core-shell particles was found to increase as the reaction temperature, time, and amount of Ti source material were increased. As-prepared core-shell particles with a smooth surface roughness were transformed into core-shell particles covered with largely grown titania crystals with different phases depending on the heat treatment temperature. The synthesis method developed in this study is a simple and economical route for the preparation of core-shell particles with various morphologies and compositions. Such particles can be employed as photoelectrical devices, catalysts, and chemical sensors.

### Acknowledgment

This work was supported by the Human Resources Development program (No. 20094020200010) of the Korea Institute of Energy Technology Evaluation and Planning (KETEP) grant funded by the Korea government Ministry of Trade, Industry and Energy.

### References

1. B. Alinec, *Colloids and Surfaces* 23 [3] (1987) 199-210.
2. Kazuhiro Akiyama, Noshio Toyama, Kazuyoshi Muraoka, and Makoto Tsunashima, *Journal of the American Ceramic Society* 81 [4] (1998) 1071-1073.
3. Nouredine Abidi, Luis Cabrales, and Eric Hequet, *ACS Appl. Mater. Interfaces* 1 [10] (2009) 2141-2146.
4. D. Garoli, M.G. Pelizzo, B. Bernardini, P. Nicolosi, and M. Alaibac, *Journal of Dermatological Science* 52 [3] (2008) 193-204.
5. Hyung Mi Sung-Suh, Jae Ran Choi, Hoe Jin Hah, Sang Man Koo, and Young Chan Bae, *Journal of Photochemistry and Photobiology, A: Chemistry* 163 [1] (2004) 37-44.
6. Yu Bai, Yiming Cao, Jing Zhang, Mingkui Wang, Renzhi Li, Peng Wang, Shaik M. Zakeeruddin, and Michael Grätzel, *Nature materials* 7 [8] (2008) 626-630.
7. Gopal K. Mor, Maria A. Carvalho, Ooman K. Varghese, Michael V. Pishko, and Craig A. Grimes, *J. Mater. Res.* 19 [2] (2004) 628-634.
8. L.A. Harris and R. Schumacher, *Journal of the Electrochemical Society* 127 [5] (1980) 1186-1188.
9. P.J. Boddy, *Journal of the Electrochemical Society* 115 [2] (1968) 199-203.
10. Richard P.N. Veregin, Maria N.V. McDougal, Carl P. Tripp, *Journal of Imaging Science and Technology* 45 [2] (2001) 174-178.
11. Suo Hon Lim, Nopphawan Phonthammachai, Stevin S. Pramana, and T.J. White, *Langmuir* 24 [12] (2008) 6226-6231.
12. Xing-Cai Guo and Peng Dong, *Langmuir* 15 [17] (1999) 5535-5540.
13. Akira Nakamura, Akira Konishi, and Sei Otsuka, *J. Chem. Soc., Dalton Trans.* [3] (1979) 488-495.
14. Suo Hon Lim, Nopphawan Phonthammachai, Ziyi Zhong, Jaelyn Teo, and T.J. White, *Langmuir* 25 [16] (2009) 9480-9486.
15. Werner Stöber, Arthur Fink, *J. Colloid Interface Sci.* 26 [1] (1968) 62-69.
16. Chen-Chi Wang and Jackie Y. Ying, *Chem. Mater.* 11 [11] (1999) 3113-3120.
17. Jingyu Wang, Xijiang Han, Wei Zhang, Zhike He, Chao Wang, Ruxiu Caib, and Zhihong Liu, *CrystEngComm* 11 [4] (2009) 564-566.
18. Jean-Pierre Jolivet, Marc Henry, and Jacques Livage in "Metal Oxide Chemistry and Synthesis: From Solution to Solid State" (Wiley-VCH Publishers, 2000) p. 83-84.
19. Zhu H.Y., Lan Y., Gao X.P., Ringer S.P., Zheng Z.F., Song D.Y., and Zhao J.C., *J. Am. Chem. Soc.* 127 [18] (2005) 6730-6736.
20. Jingyu Wang, Xijiang Han, Cheng Liu, Wei Zhang, Ruxiu Cai, and Zhihong Liu, *Cryst. Growth Des.* 10 [5] (2010) 2185-2191.